

# We are IntechOpen, the world's leading publisher of Open Access books Built by scientists, for scientists

6,900

Open access books available

186,000

International authors and editors

200M

Downloads

Our authors are among the

154

Countries delivered to

TOP 1%

most cited scientists

12.2%

Contributors from top 500 universities



WEB OF SCIENCE™

Selection of our books indexed in the Book Citation Index  
in Web of Science™ Core Collection (BKCI)

Interested in publishing with us?  
Contact [book.department@intechopen.com](mailto:book.department@intechopen.com)

Numbers displayed above are based on latest data collected.  
For more information visit [www.intechopen.com](http://www.intechopen.com)



# Vertically Aligned Carbon Nanotubes Production by PECVD

*Oleg I. Il'in, Marina V. Il'ina, Nikolay N. Rudyk,  
Alexandr A. Fedotov and Oleg A. Ageev*

## Abstract

This chapter presents the results of experimental studies of the PECVD technological mode parameters' influence on the formation of catalytic centers and carbon nanotubes' (CNTs') growth processes. This chapter also presents the ability to regulate the growth parameter for the controlled production of CNTs with the required geometric parameters, properties, and growth mechanisms. The results of experimental studies of the heating temperature and activation time effects on the catalytic center formation will be presented. This chapter also shows the effects of growth temperature, heating rate, and the activation time on the geometric and structural parameters of the carbon nanotubes. Experimental studies were carried out with the use of AFM, SEM, TEM, and EXAFS techniques. The results can be used in the development of technological processes for creating ultrafast energy-efficient electronic component base with carbon nanostructures, particularly nanoelectromechanical switches, flexo- and piezoelectric generators, gas sensors, and high-performance emitters.

**Keywords:** carbon nanotubes, PECVD, nanotechnology, technological modes, growth mechanisms

## 1. Introduction

Unique properties of carbon nanotubes (CNTs) [1–5] open wide possibilities for their application as functional elements of carbon micro- and nanoelectronics devices [6–13]. Thus, for integration of the CNT growing methods in the mass production technology, most of the interests are ordered arrays of single-walled CNT, and based on them, they are located at the place of use in accordance with the design of the developed device [14–18]. In this regard, there is necessary to provide the requirements for the structure, properties, and geometrical parameters of CNT [19].

For make requirements demanded to CNT, the plasma-enhanced chemical vapor deposition method (PECVD) is most promising [20, 21]. The initial stage of the CNTs' growing process is based on the thin layer formation of the transition metal, which are formed catalytic centers (CC) during subsequent destruction. On the surface of CC takes place dissociation of condensed carbon-containing gas molecules and transportation of free carbon atoms to the base of growing CNTs. The parameters of the catalytic centers (size, dispersion, chemical composition, etc.) [22, 23] determine the parameters of carbon nanotubes (diameter, height, chirality, electrical properties, growth kinetics, etc.) that underlie their instrument application [20, 24]. In practice, CNT arrays are most often grown on nanoscale CC obtained

by coagulation of a nanoscale thickness metal film during annealing [25, 26]. For exclusion of the interaction between the CC and the substrate, it is necessary to form buffer layers based on metal or dielectric films.

In the PECVD method, there are a lot number of interrelated parameters (temperature, pressure, gas flows, gas types, types of catalyst film material, etc.) that influence the processes of CC formation and CNT growth [27, 28].

This chapter describes the results of experimental research of the PECVD technological modes that influence on the formation of CC and vertically aligned carbon nanotubes' (VA CNTs') growth for the controlled production of nanotubes with the required geometric parameters and properties.

## **2. Features of the PECVD process parameters' influence on the formation of catalytic centers and carbon nanotubes' growth**

### **2.1 Experimental samples and equipment**

Experimental research on the formation of catalytic centers and the growth of VA CNT was performed using the PECVD module of cluster nanotechnology complex NANOFAB NTK-100 (NT-MDT, Russia). A silicon wafer with a deposited chromium film and a nickel catalytic film with thicknesses of 20 and 10 nm, respectively, was used as the initial substrate. Cr and Ni films were deposited by magnetron sputtering on an AUTO 500 (BOC Edwards, UK). The catalytic centers formation was performed in an argon and ammonia atmosphere. The CNT growth was performed in ammonia and acetylene atmosphere. In all experimental researches, the pressure in the chamber was 4.5 Torr. The structural analysis of the VA CNT arrays was conducted by the transmission electron microscopy (TEM) using the Tecnai Osiris (FEI, Netherlands) and the Raman spectrometer Renishaw InVia Reflex (Renishaw plc, UK). Analysis of TEM images and Raman spectra showed that the experimental samples were multiwalled carbon nanotubes [29]. Surface investigations of the obtained VA CNT arrays were carried out using a scanning electron microscope (SEM) Nova Nanolab 600 (FEI Company, Netherlands). Investigation of structure and analysis of processes in catalyst films and sublayer was performed by extended X-ray absorption fine structure spectroscopy (EXAFS) with special source of synchrotron radiation (Kurchatov Institute, Russia). Analysis of geometric parameters of CC was conducted by atomic force microscopy using the Ntegra Probe Nanolaboratory (PNL) (NT-MDT, Russia). To process the experimental data, the ImageAnalysis application package was used.

### **2.2 The effect of heating temperature on the catalytic center formation**

As a catalyst for growing CNT, most often used transition metals are Fe [30–34], Ni [35, 36], Co [37–39], and binary compounds based on them such as Fe-Mo [40], Co-Fe [41], Fe-Cu [42]. At the same time, an important factor to create devices with CNTs is the growth of nanotubes on the sublayer ohmic contact. This factor creates additional difficulties in technological process by increasing kinetic interactions at high growth temperatures, such as doping and formation of intermetallic compounds between the catalyst and the sublayer material.

Experimental research was performed on the samples with Ni/Cr/Si structure. The samples were heated in the temperature range 700–800 with 50°C interval in PECVD module in the atmosphere of inert gas ( $Q_{Ar} = 40$  sccm) and ammonia ( $Q_{NH_3} = 15$  sccm). Argon is used to purge the chamber and remove residual air.

Ammonia creates a reducing atmosphere in the reactor that prevents oxidation of the catalytic film. During the annealing fragmentation and corrugating, Ni film occurs with catalytic centers formation.

On the initial samples, according to the SEM data, the surface of the structure was smooth. After heating the samples to a given temperature, the metal film was fragmented with CC formation (**Figure 1**).

Analysis and statistical processing of the obtained AFM images allowed to obtain the dependence of the catalytic centers height and diameter by substrate heating temperature (**Figure 2**).

From the obtained dependences (**Figure 2**), it can be seen that the heating temperature has a significant effect on the geometric dimensions of the CC. The difference between the temperature expansion coefficients of Si substrate ( $10.9 \times 10^{-6} \text{C}^{-1}$ ) and Cr sublayer film ( $3.1 \times 10^{-6} \text{C}^{-1}$ ) promotes the appearance of significant mechanical stresses during annealing in the film/substrate contact, which causes fragmentation and rupture of the metal film into separate islands. CC formed at a temperature of  $700^\circ\text{C}$  is characterized by a larger scatter of geometric parameters, which is associated with the initiation of the film breakdown process and insufficiently intense surface diffusion of Ni atoms. As the temperature rises to  $750^\circ\text{C}$ , diffusion exchange of atoms is activated through the contact plane between the film and the substrate. As the plasticity of the metal increases, the consolidation of small CC into larger ones with a decrease in the scatter of their height is observed.

When the temperature rises above  $750^\circ\text{C}$ , a simultaneous process of sublimation and surface diffusion is observed, which leads to a decrease in the diameter and height of the CC. At the same time, there is a decrease in the number of small CCs, which were observed at a temperature of  $700^\circ\text{C}$ .

To analyze the processes occurring in the films of the catalyst and the sublayer during heating, the sample with  $750^\circ\text{C}$  heated temperature was investigated by EXAFS. The obtained X-ray absorption spectra (**Figure 3**) were compared with spectra of the reference substrates.

The results of the research show that in the Ni/Cr/Si structure, Ni is mainly in the oxidized state (the volume of pure Ni is  $\sim 30\%$ ). The Cr absorption spectrum (**Figure 3b**) coincides with the reference spectrum of  $\text{Cr}_2\text{O}_3$ .

For the subsequent growth of CNTs, it is necessary to form QC from pure Ni; therefore, it is necessary to carry out the process of “activation” (i.e., reduction) of Ni from NiO before synthesizing CNTs.

This research was supported by the Russian Science Foundation under grant no. 18-79-00176.

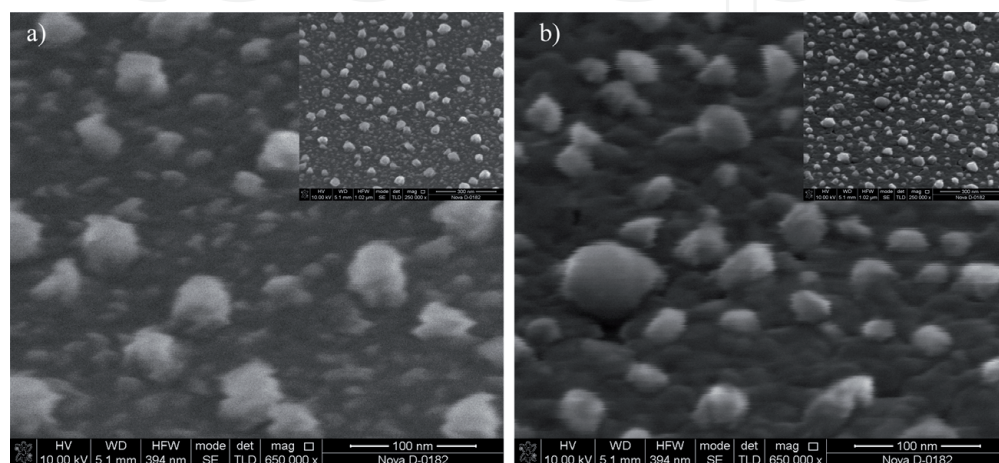


**Figure 1.**  
SEM images of CC formed at different heating temperatures: (a)  $700^\circ\text{C}$ , (b)  $800^\circ\text{C}$ .



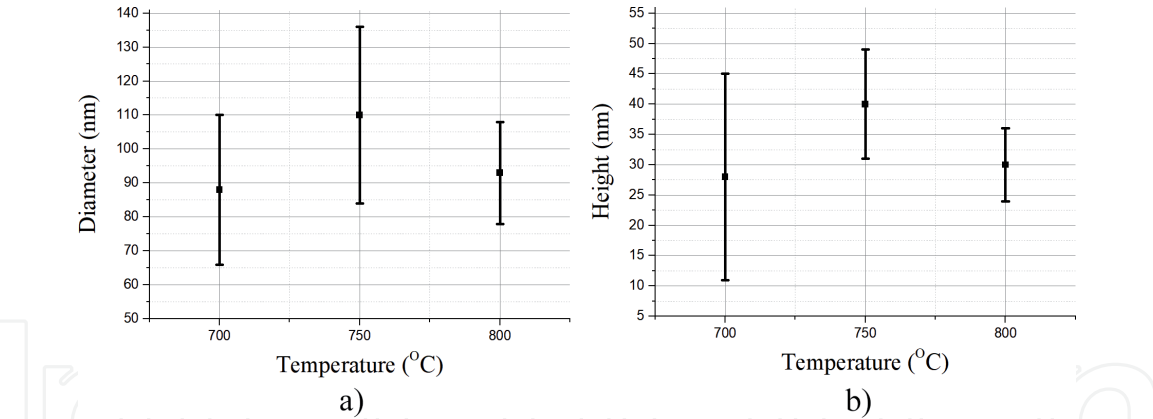


**Figure 2.** Dependencies of diameter (a) and height (b) from the substrate heating temperature.

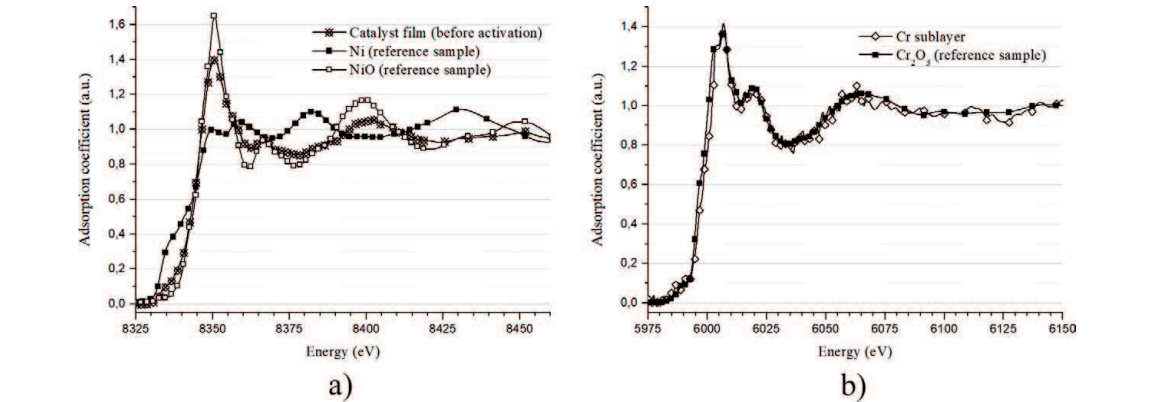


**Figure 3.** EXAFS spectra of Ni/Cr/Si structures after baking at the heating stage, for the absorption energy range of Ni (a) and Cr (b).

2.3 The effect of activation time on the catalytic center formation

The ammonia gas line in the PECVD module allows for the “activation” process. “Activation” is the exposure of samples in an NH<sub>3</sub> atmosphere (210 sccm) obtained at the heating stage. The use of a DC high-voltage source allows to initiate the plasma at the “activation” stage. To analyze the effect of “activation” stage on the catalytic center parameters, a series of experiments were carried out to determine the dependence of the effect of exposure time in ammonia with and without plasma initiation.

In the beginning, experimental samples were created at the heating stage (heating to 750°C for 20 min, in an atmosphere of Ar (40 sccm) and NH<sub>3</sub> (15 sccm)). Upon completion of the heating stage, the “activation” stage began. Only NH<sub>3</sub> (210 sccm) was fed into the chamber, while the heating temperature did not change. The exposure time of the samples was 1, 3, and 5 min. Sample nos. 1–3 were exposed without plasma initiation, nos. 4–6 with initiation ammonia plasma.

Research of CC parameters was provided by AFM and SEM. The results of numerical processing AFM images are present on **Figure 4**.

Based on the data obtained, it can be concluded that the “activation” process has a significant impact on the evolution of catalytic centers. Moreover, the greatest contribution is made by the impact time and not by the presence of plasma in the process.

Comparison of dependencies of **Figures 2** and **4** shows that exposure in ammonium atmosphere leads to additional etching of Ni CC and reducing their diameter and height. At the activation stage are formed more ordered and uniform CC arrays in comparison with arrays obtained at the heating stage. It is shown that an increase

in the processing time of a CC at the “activation” stage allows not only to reduce the CC sizes from  $122 \pm 19$  to  $65 \pm 9$  nm (in the 1–5 min exposure time range), but also to increase their homogeneity.

Investigation of the activation process effect on the reduction of NiO to Ni was not carried out due to possible oxidation of CC during the chamber vacuum is released.

This study was supported by the Russian Science Foundation under grant no. 18-79-00176.

#### 2.4 The effect of growth temperature on carbon nanotubes geometric dimensions

The growth stage is a technological step which begun after the “activation” stage. Into the chamber of the PECVD module a mixture of NH<sub>3</sub> (210 sccm) and C<sub>2</sub>H<sub>2</sub> (70 sccm) gases is fed. Plasma is initiated for the vertical alignment of CNT relative to the substrate in the growth process.

SEM images of the grown CNTs are present in **Figure 5**. Due to the features of the CNTs growing process in PECVD module, set temperature in the heating step also serves “activation” and growth temperatures.

The SEM images show the integral temperature effect, which is associated both with the formation of CC at the stages of heating and activation, and with the CNT growth processes at set temperature. For samples obtained at a temperature of 650°C, characterized by the height of the CNT array  $65 \pm 5$  nm, with a diameter of  $25 \pm 3$  nm and the presence of disoriented CNTs. CNTs are grown by the “tip” mechanism. Increasing the temperature to 700°C leads to the elimination of the formation of disoriented CNTs and CNT geometric dimensions are in the same range (diameter  $25 \pm 4$  nm, height  $66 \pm 5$  nm). This effect may be associated with better hydrogen desorption in the decomposition of acetylene on CC surface. This leads to the formation of a less “defective” carbon layer on the CC surface, which does not give branching and disorientation of CNT. A raise temperature to 750°C leads to an increase in the mobility of the CC and association smaller CC into larger. The parameters of CNT were: diameter  $44 \pm 3$  nm and height  $80 \pm 9$  nm. Also observed growth of individual CNTs with a diameter of  $70 \pm 3$  nm and height  $350 \pm 10$  nm. At 800°C diameter and height of CNT arrays were  $51 \pm 6$  nm and  $100 \pm 12$ , respectively. There is also observed of individual CNT with a height of  $600 \pm 24$  nm and diameter of  $52 \pm 6$  nm. The observed with increasing temperature, raising CNT diameter indicating continued association small CC into larger in heating and activation stages. The almost complete absence of CNTs with a diameter of less than 25 nm indicates

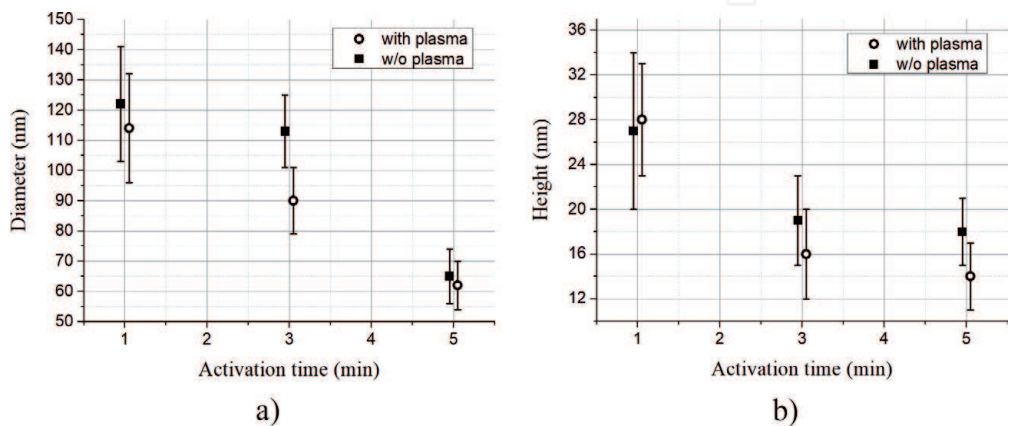


**Figure 4.**  
Dependencies of diameter (a) and height (b) on time of activate.

the ongoing process of absorption of small CC by larger ones or possible sublimation of small CC at a given temperature. However, with increasing temperature the process of acetylene desorption from the sample surface is accelerated. Thus, not having time to react with the CC carbon-containing gas is pumped out by vacuum system.

Structural analysis of the VA CNT arrays grown at temperatures of 700, 750, and 800°C was carried out using the Raman spectroscopy (**Figure 6**).

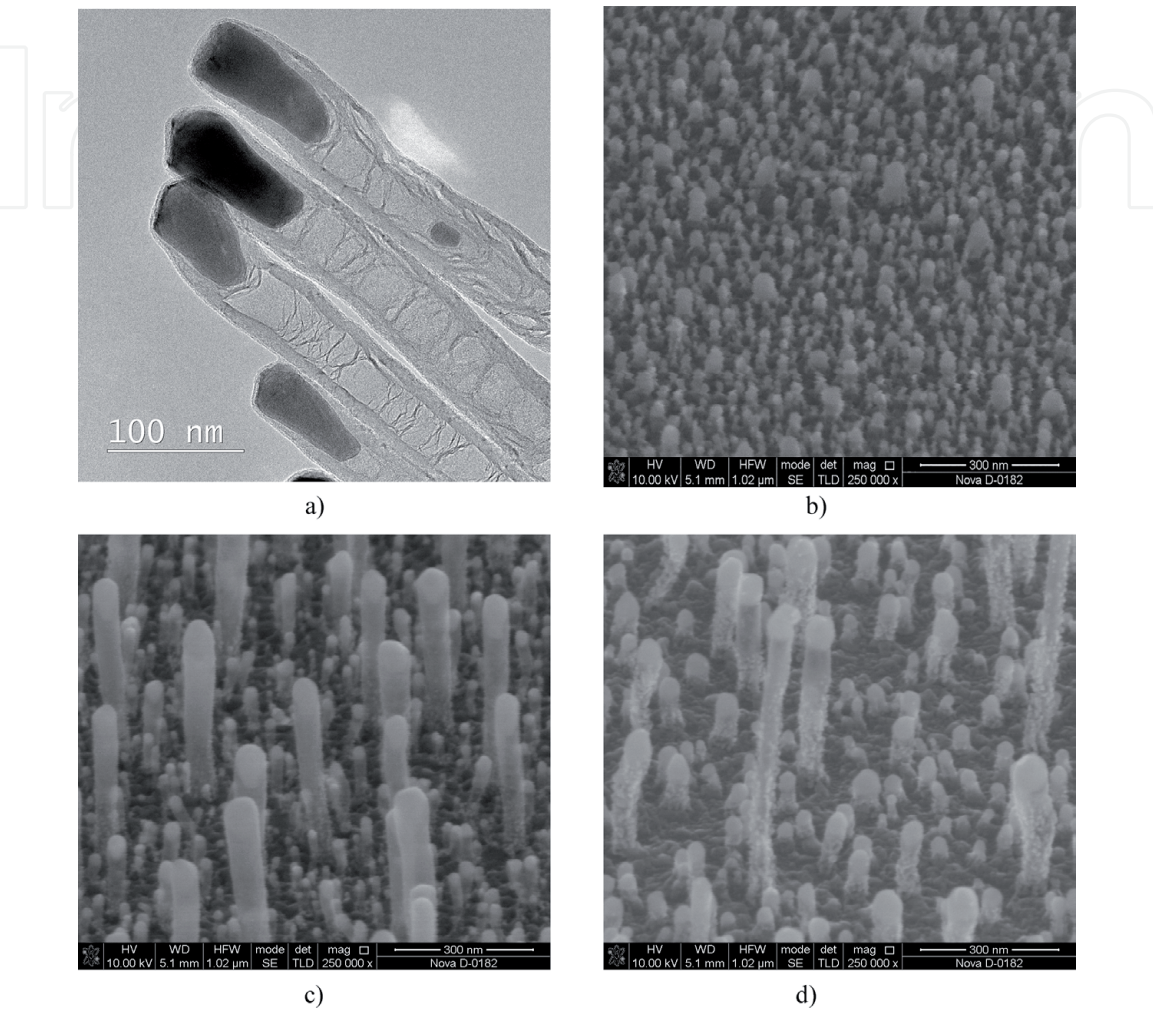


**Figure 5.** Images of VA CNT arrays obtained at different growth temperatures: (a) TEM image, 750°C; and SEM images: (b) 700°C; (c) 750°C; (d) 800°C.

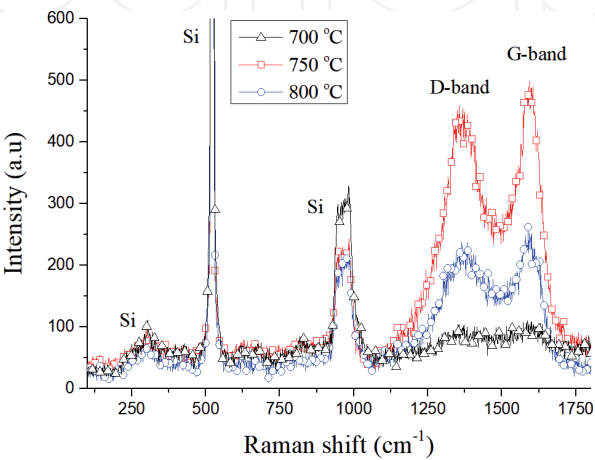


**Figure 6.** Raman spectra of the VA CNT arrays grown at different temperatures.



The absence of the RBM mode in the range of 0–200  $\text{cm}^{-1}$  and the presence of D- and G-modes on the spectrum shows that the grown CNTs are multiwalled. The ratio of the peaks  $I_D/I_G$  shows that the defectiveness of the tubes is 0.91, 0.88 and 0.90 for growth temperatures of 700, 750 and 800°C, respectively. High “defects” of CNT is related with the features of samples structure and technique for obtaining the spectra at which the laser beam falls along the normal to the substrate surface. The presence of Ni CC in the top of the CNTs can lead to an increase in the amplitude of the D-mode and, as a result, cause symmetry breaking of the graphite layer with  $\text{sp}^2$  hybridization of carbon atoms, which is recorded in the spectrum. However, a comparative analysis found that CNT obtained at a temperature of 750°C characterized by the lowest “defectiveness”. The ratio of the amplitude of the main mode of Si to the G-mode of a CNT qualitatively shows that the concentration of CNTs grown at a temperature of 750°C is 3.1% and 5.2% higher than that of samples grown at 800 and 700°C, respectively.

CNTs grown at a temperature of 750°C were investigated using EXAFS. X-ray absorption spectra are shown in **Figure 7**.

The EXAFS results show that Ni on CNT samples have almost completely recovered, with a metal percentage of 90–95%. A decrease in the spectrum intensity of the chromium absorption energy range of a sample with CNT (**Figure 7b**) compared to a sample with CC (**Figure 3b**) suggests the presence of a phase transformation of  $\text{Cr}_2\text{O}_3$  to CrO, or the formation of a solid solution of  $\text{Cr}_2\text{O}_3 + \text{Cr}_3\text{C}_2$ . The reduction of the oxidized chromium sublayer to metallic Cr does not occur at the all stages of PECVD process. A comparative analysis of the diameter of CC formed at the end of the “activation” stage and the diameter of grown CNTs allows to conclude that CC with a diameter of less than 70–90 nm produce growth of single CNTs.

This study was supported by the Russian Science Foundation under grant no. 18-79-00176.

## 2.5 Effect of heating rate on the carbon nanotube parameters

To investigate the effect of heating rate on the geometric dimensions of CNTs, a series of experiments on heating samples to temperatures of 650, 750, and 800°C in 20 and 45 min were carried out (**Figure 8**).

Based on the data obtained from SEM images (**Figure 9**), it can be concluded that at low heating temperatures (650°C), the heating rate does not have a significant impact on the parameters of the grown CNTs.

In sample nos. 1 and 2, the CNTs diameter was about 30 nm and height about 45 nm. When the temperature rises to 750°C in sample no. 3, compared with nos. 1 and 2, there is an increase of CNTs height ( $300 \pm 35$  nm) and diameter ( $54 \pm 8$  nm). An increase in heating time to 45 min (sample no. 4) leads to a decrease in the dispersion of the CCs diameter at the heating stage. The CNT arrays on sample no. 4 have a greater homogeneity of nanotubes (as compared with samples No 3), and diameter was  $45 \pm 4$  nm and height  $280 \pm 30$  nm. These geometrical dimensions indicate the absorption of small CCs by large CCs at the heating and activation stages, with the subsequent sublimation of CCs. Heating the sample no. 5 to 800°C in 20 min allowed to form CNT arrays with diameter of  $60 \pm 7$  nm and height of  $120 \pm 10$  nm. Separate CNTs with heights up to 600 nm were observed. A decrease in the sample no. 6 heating rate (800°C for 45 min) leads to the formation of CNTs with a diameter of  $65 \pm 6$  nm and a height of  $85 \pm 10$  nm. It can be assumed that at a temperature of 800°C, an increase in CC formation time leads to raising in the number of silicon atoms “jumps” and their exit through the  $\text{Cr}_x\text{Si}_y/\text{Cr}$  layer to nickel CCs. In this case, Ni interacts well with Si with formation of nickel silicides, which causes a decrease in the catalytic activity of Ni. An increase in the heating time to



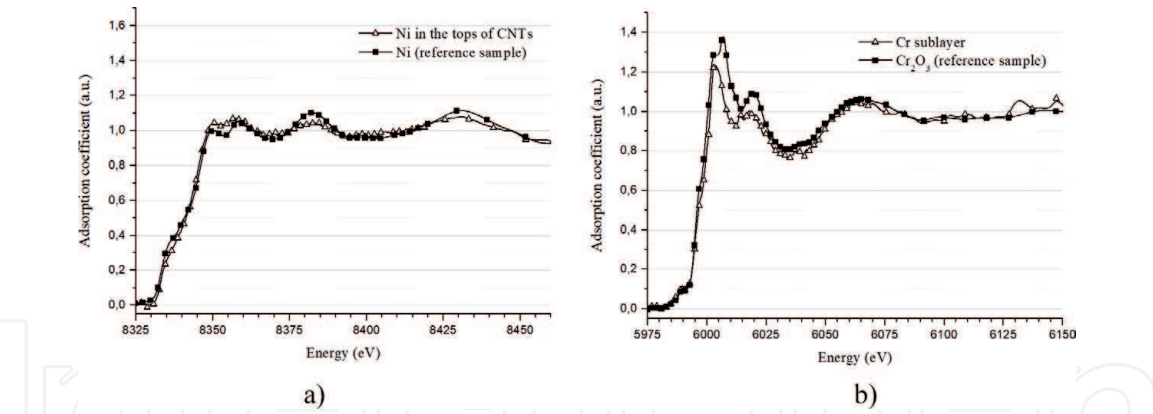


**Figure 7.** EXAFS spectra of Ni/Cr/Si structure after growth process for the absorption energy range of Ni (a) and Cr (b).

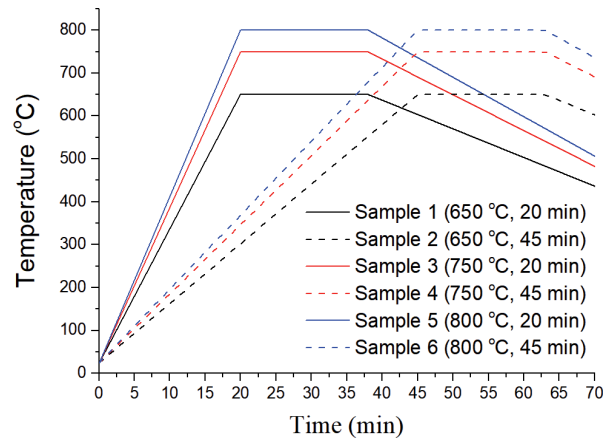


**Figure 8.** Schematic representation of the CNT growing process on samples with different heating rates.

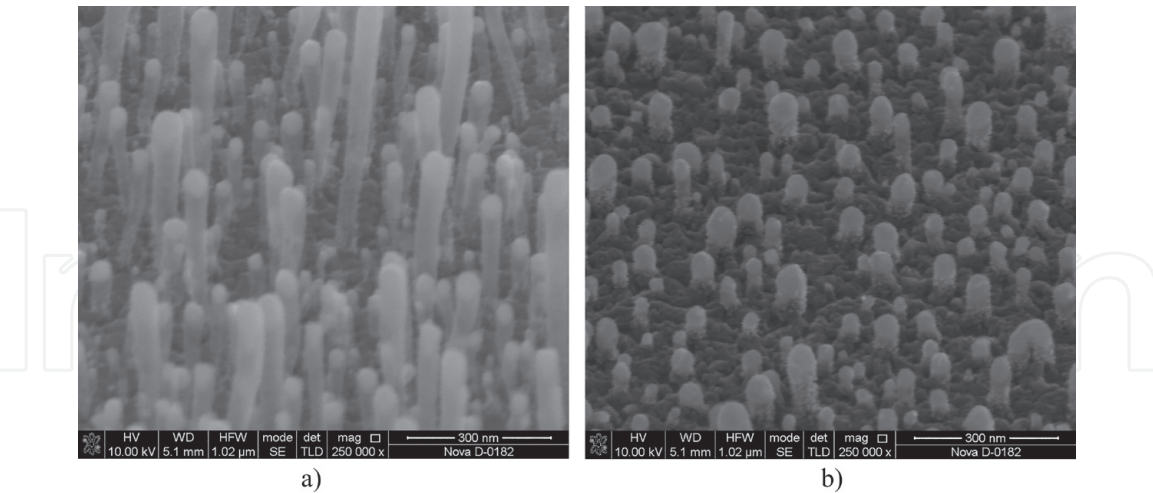


**Figure 9.** SEM images of substrates with CNT heated for 45 min to temperatures: (a) 750°C, (b) 800°C.

45 min becomes sufficient to saturate nickel CCs with silicon, and a temperature of 800°C leads to a better dissolution of carbon in the poisoned CC. As a result, CC is oversaturated by carbon, with subsequent carbidization of the catalyst and stopping the growth process.

It should be noted that heating above 650°C does not have a significant effect on the diameter of the grown CNTs. However, control of the heating rate and growth temperature allows stabilizing the height of the CNT at  $280 \pm 30$  nm and reducing the variation of nanotube diameters.

2.6 The effect of activation time on the carbon nanotube parameters

To investigate the effect of the activation process on the CNTs growth without plasma, the values of diameter, height, and density of CNT for all samples were determined in [27] (**Table 1**).

An increase in the diameter and a decrease density of CNTs at intervals of 1–3 and 6–10 min is associated with the predominance of the absorption processes of small centers with large centers. But at the time intervals of 3–6 and 10–15 min, the etching processes of CC in the ammonia atmosphere prevail. At the same time, the intervals of 3–6 and 10–15 min are dominated by the processes of CC etching in the ammonia atmosphere. All obtained CNTs are grown by the “top” mechanism. It should be noted that when the activation time is more than 1 min, the CNTs in the growth process begin to unite into bundles, which is not observed when CC is activated in the plasma. With an increase in the activation time, a decrease in the deviation of the growing tubes from the normal to the substrate is observed.

To assess the effect of the growth process on the parameters of CNT, an experiment without the “activation” stage was conducted. SEM images of the obtained CNTs are shown in **Figure 10**.

From **Figure 10**, it can be seen that the CNTs obtained without “activation” stage are grown by the “root” mechanism, and the open CNTs peaks begin to branch with graphite flakes formation. Thus, control of the activation process allows to control CNT growth mechanism.

2.7 The effect of growth time on the carbon nanotube parameters

To research the growth time effect on the geometrical dimensions of CNTs, samples with CNTs, whose growth time was 5, 10, 15, and 30 min, were investigated by [28].

As a result of processing the obtained SEM images (**Figure 11**), the dependences of the diameter and height of the CNT on the growth time (**Figure 12**) are shown.

From the obtained dependences (**Figure 12**), it is seen that with an increase in the growth time to 15 min, the diameter and height of the CNT vary linearly with time. In the interval of growth from 15 to 30 min CNTs diameter does not change significantly, and the height dependence has a tendency to saturate. Thus, it can be assumed that in the initial stages simultaneously with the increase in length, the formation of new walls of CNTs occurs, which leads to an increase in the external diameter of the nanotubes. When in these technological modes the critical size of the CNT is reached, the disorientation of the CNTs begins (**Figure 11c**).

The investigation of CNTs by the Raman spectroscopy (**Figure 13**) showed that the spectra of CNTs grown within 5 min are almost the same as the spectra of CNTs grown within 10 min. CNTs grown for 15 min show a noticeable

Activation time, min	CNTs' diameter, nm	CNTs' height, nm	CNTs' density, mkm <sup>-1</sup>
1	26 ± 4	77 ± 8	410 ± 38
3	35 ± 8	250 ± 20	250 ± 25
6	24 ± 4	200 ± 9	171 ± 18
10	51 ± 11	260 ± 22	136 ± 16
15	50 ± 5	310 ± 25	228 ± 23

**Table 1.**  
*Parameters of CNT grown at different activation time.*



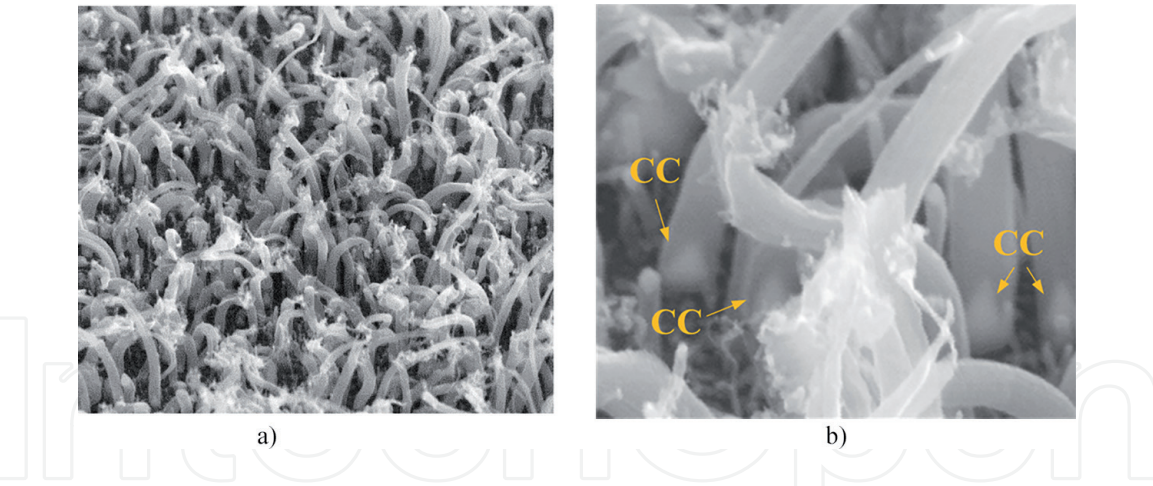


**Figure 10.**  
CNT arrays grown without activation at different magnification: (a) 40000 $\times$ , (b) 200000 $\times$ .

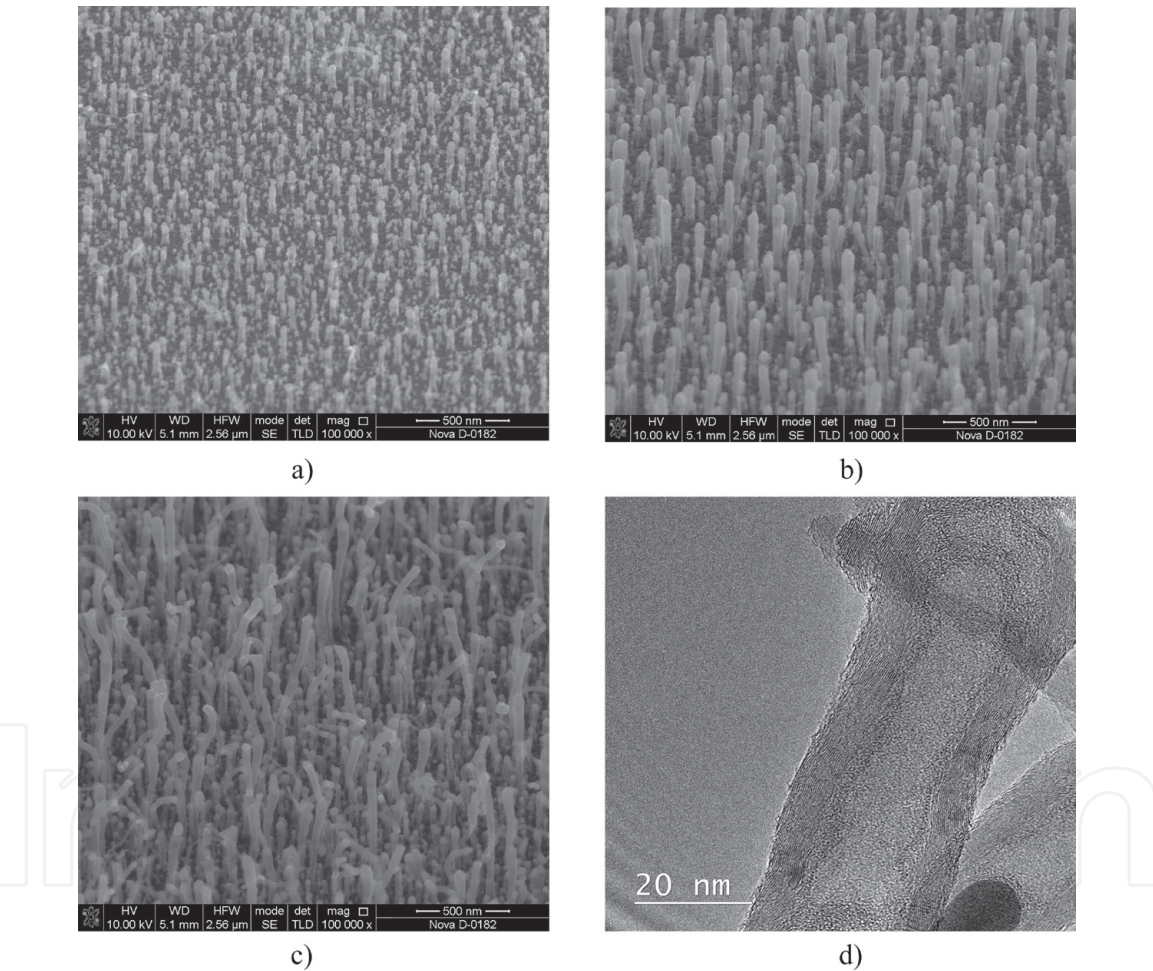


**Figure 11.**  
SEM images of CNT grown at different time: (a) 5 min, (b) 15 min, (c) 30 min, and (d) TEM image (15 min).

increase in the intensity of the spectrum. That is, an increase in the height of the CNT leads to an increase in Raman intensity. The ratio of  $I_D/I_G$  peaks was found to be 0.95, 0.86, and 0.91 for growth times of 5, 10, and 15 min, respectively. The high “defectiveness” of CNTs grown within 5 min is explained by the small height and diameter of CNTs, where most of the volume of CNTs is the catalytic center, which makes a large contribution to the intensity of the D-mode.

With a raised growth time of 10 min, an increase in the aspect ratio and a decrease in “defects” of CNTs are obtained. However, a further increase in growth time causes the process of undercutting of the base of a CNT by plasma



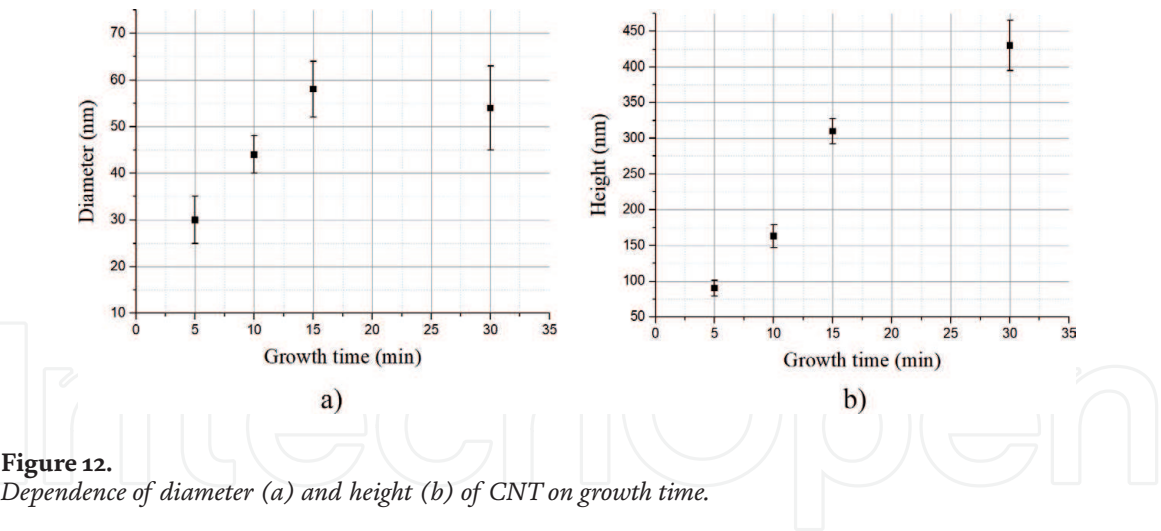


**Figure 12.**  
Dependence of diameter (a) and height (b) of CNT on growth time.

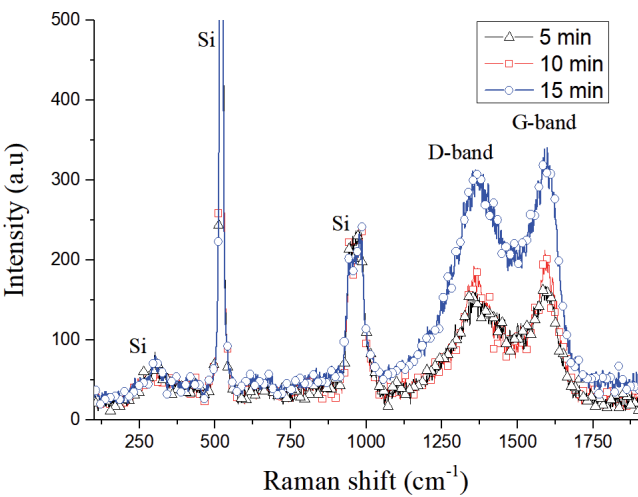


**Figure 13.**  
Raman spectra of the VA CNT arrays with 5, 10, and 15 min grown time.

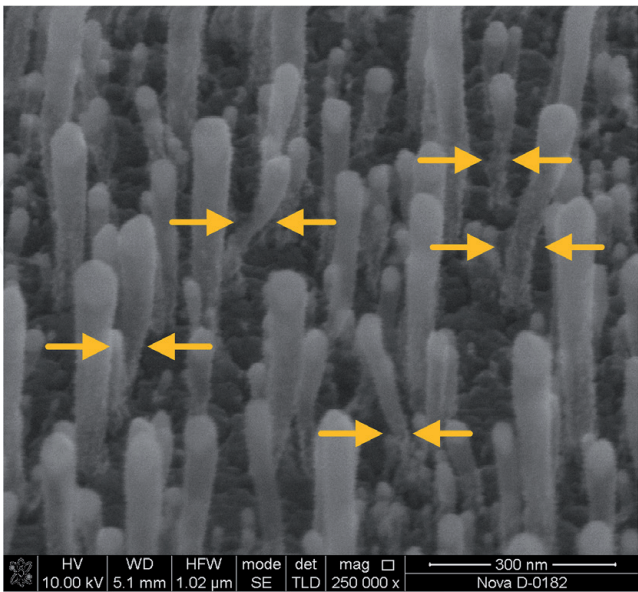


**Figure 14.**  
CNTs grown for 15 min.

(Figure 14). The processing time in plasma increases with increasing time of growth itself, which leads to disruption of carbon bonds and the growth of the D-mode in Raman spectra.

Thus, the growth time has a significant impact on both the height of the CNTs and their “defectiveness.” Therefore, to obtain CNTs of greater height with less “defectiveness,” it is necessary to select modes with lower plasma power or growth time, as well as increase the pressure of carbon-containing gas to accelerate the transport of acetylene to the CCs.

This study was supported by the Russian Science Foundation under grant no. 18-79-00176.

### 3. Conclusion

As a result of the performed research, the PECVD modes of production CC with controlled parameters were determined. It is shown that heating at a temperature of 700–800°C, with simultaneous inlet of argon and ammonia into the PECVD chamber, makes it possible to obtain CCs with a diameter of  $110 \pm 11$  nm and a height of  $40 \pm 7$  nm. It was established that ammonia at the “activation” stage allows reducing the diameter (up to  $90 \pm 18$  nm) and height (up to  $18 \pm 3$  nm), as well as increasing the homogeneity of the array of the obtained catalytic centers. It was confirmed that on the heating stage, Ni CCs are in an oxidized state with an Ni content of ~30%, but Ni is reduced to almost pure metal (95%) at the “activation” stage.

It is established that the growth temperature of 750°C shows the smallest “defectiveness” of CNTs with a diameter of  $44 \pm 3$  nm and a height of  $80 \pm 9$  nm. It is shown that at low temperatures (650°C), the heating rate does not have a significant impact on the parameters of the grown CNTs, herewith diameter and height of the CNT was about 30 and 45 nm, respectively. Heating above 650°C does not affect the diameter of the obtained CNT; however, control of the heating rate and growth temperature allows stabilizing the height of the CNT at  $280 \pm 30$  nm with a diameter of  $45 \pm 4$  nm.

The PECVD modes of growth CNTs with controlled “tip” and “root” mechanisms are determined. It was established that the control of technological parameters at the “activation” stage allows to control the diameter ( $24 \pm 4 - 51 \pm 11$  nm) and density ( $136 \pm 16 - 410 \pm 38 \mu\text{m}^{-2}$ ) of CNTs.

The obtained results can be used in the development of technological processes for the creation of ultrafast energy-efficient electronic components based on carbon nanostructures, particularly nanoelectromechanical switches [43, 44], flexo- and piezogenerators [45, 46], gas sensors [47, 48], and highly efficient autoelectronic emitters [49, 50].

### Acknowledgements

Chapter paragraphs 2.2–2.4 and 2.7 were supported by the Russian Science Foundation under grant no. 18-79-00176.

Chapter paragraphs 2.5 and 2.6 were financially supported by the Russian Foundation for Basic Research (project no. 16-29-14023 ofi\_m) and Internal grant of the Southern Federal University (project no. VnGr-07/2017-26).

### Conflict of interest

The authors declare no conflict of interest.

## Thanks

The authors are grateful to Zubavichus Ya.V. (NRC “Kurchatov Institute”) for research and interpretation of the obtained EXAFS spectra and to Levshov D.I. (Southern Federal University) for assistance in research by Raman spectroscopy.

## Author details

Oleg I. Il'in<sup>1\*</sup>, Marina V. Il'ina<sup>1</sup>, Nikolay N. Rudyk<sup>1</sup>, Alexandr A. Fedotov<sup>1</sup> and Oleg A. Ageev<sup>2</sup>

<sup>1</sup> Institute of Nanotechnologies, Electronics and Electronic Equipment Engineering, Southern Federal University, Taganrog, Russian Federation

<sup>2</sup> Research and Education Center “Nanotechnologies”, Southern Federal University, Taganrog, Russian Federation

\*Address all correspondence to: [oiilin@sfedu.ru](mailto:oiilin@sfedu.ru)

## IntechOpen

© 2019 The Author(s). Licensee IntechOpen. This chapter is distributed under the terms of the Creative Commons Attribution License (<http://creativecommons.org/licenses/by/3.0>), which permits unrestricted use, distribution, and reproduction in any medium, provided the original work is properly cited. 



## References

- [1] Lim YD, Grapov D, Hu L, et al. Enhanced field emission properties of carbon nanotube bundles confined in SiO<sub>2</sub> pits. *Nanotechnology*. 2018;**29**(7):075205. DOI: 10.1088/1361-6528/aaa1bb
- [2] Wang J, Jin X, Liu Z, et al. Growing highly pure semiconducting carbon nanotubes by electrotwisting the helicity. *Nature Catalysis*. 2018;**1**(5): 326-331. DOI: 10.1038/s41929-018-0057-x
- [3] Lutz C, Ma Z, Thelen R, et al. Analysis of carbon nanotube arrays for their potential use as adhesives under harsh conditions as in space technology. *Tribology Letters*. 2019;**67**(1):10. DOI: 10.1007/s11249-018-1121-z
- [4] Syurik J, Ageev OA, Cherednichenko DI, Konoplev BG, Alexeev A. Non-linear conductivity dependence on temperature in graphene-based polymer nanocomposite. *Carbon*. 2013;**63**:317-323. DOI: 10.1016/j.carbon.2013.06.084
- [5] Il'ina M, Il'in O, Blinov Y, Konshin A, Konoplev B, Ageev O. Piezoelectric response of multi-walled carbon nanotubes. *Materials (Basel)*. 2018;**11**(4):638. DOI: 10.3390/ma11040638
- [6] Bokobza L. Multiwall carbon nanotube elastomeric composites: A review. *Polymer (Guildf)*. 2007;**48**(17):4907-4920. DOI: 10.1016/j.polymer.2007.06.046
- [7] De Volder MFL, Tawfick SH, Baughman RH, Hart AJ. Carbon nanotubes: Present and future commercial applications. *Science (80-)*. 2013;**339**(6119):535-539. DOI: 10.1126/science.1222453
- [8] Franklin AD, Luisier M, Han S-J, et al. Sub-10 nm carbon nanotube transistor. *Nano Letters*. 2012;**12**(2): 758-762. DOI: 10.1021/nl203701g
- [9] Lim YD, Hu L, Avramchuck AV, et al. Temperature-dependent selective growth of carbon nanotubes in Si/SiO<sub>2</sub> structures for field emitter array applications. *Materials Research Bulletin*. 2017;**95**:129-137. DOI: 10.1016/j.materresbull.2017.07.022
- [10] Peng H, Li Q, Chen T, editors. *Industrial Applications of Carbon Nanotubes*. A volume in: *Micro and Nano Technologies*. Amsterdam: Elsevier; 2017. DOI: 10.1016/C2015-0-00493-2. Available from: <https://www.sciencedirect.com/book/9780323414814/industrial-applications-of-carbon-nanotubes>
- [11] Alekseev A, Chen D, Tkalya EE, et al. Local organization of graphene network inside graphene/polymer composites. *Advanced Functional Materials*. 2012;**22**(6):1311-1318. DOI: 10.1002/adfm.201101796
- [12] Syurik YV, Ghislandi MG, Tkalya EE, et al. Graphene network organisation in conductive polymer composites. *Macromolecular Chemistry and Physics*. 2012;**213**(12):1251-1258. DOI: 10.1002/macp.201200116
- [13] Sanchez Esqueda I, Yan X, Rutherglen C, et al. Aligned carbon nanotube synaptic transistors for large-scale neuromorphic computing. *ACS Nano*. 2018;**12**(7):7352-7361. DOI: 10.1021/acsnano.8b03831
- [14] Bonard J-M, Croci M, Klinke C, Kurt R, Noury O, Weiss N. Carbon nanotube films as electron field emitters. *Carbon*. 2002;**40**(10):1715-1728. DOI: 10.1016/S0008-6223(02)00011-8
- [15] Zou J, Zhang K, Li J, et al. Carbon nanotube driver circuit for 6 × 6 organic

light emitting diode display. Scientific Reports. 2015;5(1):11755. DOI: 10.1038/srep11755

[16] Tolt ZL, McKenzie C, Espinosa R, Snyder S, Munson M. Carbon nanotube cold cathodes for application in low current x-ray tubes. Journal of Vacuum Science & Technology B: Microelectronics and Nanometer Structures. 2008;26(2):706. DOI: 10.1116/1.2802092

[17] Heo S, Kim H, Ha J, Cho S. A vacuum-sealed miniature X-ray tube based on carbon nanotube field emitters. Nanoscale Research Letters. 2012;7(1):258. DOI: 10.1186/1556-276X-7-258

[18] Park S, Vosguerichian M, Bao Z. A review of fabrication and applications of carbon nanotube film-based flexible electronics. Nanoscale. 2013;5(5):1727. DOI: 10.1039/c3nr33560g

[19] Levchenko I, Han Z-J, Kumar S, Yick S, Fang J, Ostrikov K. Large arrays and networks of carbon nanotubes: Morphology control by process parameters. In: Syntheses and Applications of Carbon Nanotubes and Their Composites. IntechOpen. London, UK; 2013. DOI: 10.5772/52674

[20] Tanaka K, Iijima S, editors. Carbon Nanotubes and Graphene. 2nd ed. Amsterdam: Elsevier; 2014. DOI: 10.1016/C2011-0-07380-5. Available from: <https://www.sciencedirect.com/book/9780080982328/carbon-nanotubes-and-graphene#book-info>

[21] Ageev OA, Balakirev SV, Bykov AV, et al. Development of new metamaterials for advanced element base of micro- and nanoelectronics, and microsystem devices. In: Advanced Materials. Springer Proceedings in Physics. Springer International Publishing Switzerland. 2016;563-580. DOI:10.1007/978-3-319-26324-3\_40

[22] Bulyarskii SV, Basaev AS. Coalescence of clusters of catalysts for the growth of carbon nanotubes during their formation under homogeneous and heterogeneous conditions. Physics of the Solid State. 2015;57(6):1055-1059. DOI: 10.1134/S1063783415060074

[23] Fedotov AA. Study of growth processes of PECVD carbon nanotubes, used in micro- and nanosystem technologies. In: Piezoelectrics and Nanomaterials: Fundamentals, Developments and Applications. Nova Science Publishers, Inc. New York, USA; 2015. pp. 61-84

[24] Gao J, Zhong J, Bai L, Liu J, Zhao G, Sun X. Revealing the role of catalysts in carbon nanotubes and nanofibers by scanning transmission X-ray microscopy. Scientific Reports. 2015;4(1):3606. DOI: 10.1038/srep03606

[25] Neyts EC. The role of ions in plasma catalytic carbon nanotube growth: A review. Frontiers of Chemical Science and Engineering. 2015;9(2):154-162. DOI: 10.1007/s11705-015-1515-5

[26] Shariat M, Shokri B, Neyts EC. On the low-temperature growth mechanism of single walled carbon nanotubes in plasma enhanced chemical vapor deposition. Chemical Physics Letters. 2013;590:131-135. DOI: 10.1016/j.cplett.2013.10.061

[27] Il'in OI, Il'ina MV, Rudyk NN, Fedotov AA, Levshov DI, Ageev OA. The influence of activation and growth time on the geometry and structural perfection of multi-walled carbon nanotubes. Journal of Physics Conference Series. 2018;1038:012062. DOI: 10.1088/1742-6596/1038/1/012062

[28] Il'in OI, Il'ina MV, Rudyk NN, Fedotov AA, Ageev OA. The growth temperature effect on vertically aligned carbon nanotubes parameters.

- Nanosystems: Physics, Chemistry, Maths. 2018;**9**(1):92-94. DOI: 10.17586/2220-8054-2018-9-1-92-94
- [29] Il'ina MV, Il'in OI, Blinov YF, et al. Memristive switching mechanism of vertically aligned carbon nanotubes. Carbon. 2017;**123**:514-524. DOI: 10.1016/j.carbon.2017.07.090
- [30] Amama PB, Pint CL, McJilton L, et al. Role of water in super growth of single-walled carbon nanotube carpets. Nano Letters. 2009;**9**(1):44-49. DOI: 10.1021/nl801876h
- [31] de los Arcos T, Garnier MG, Seo JW, Oelhafen P, Thommen V, Mathys D. The influence of catalyst chemical state and morphology on carbon nanotube growth. The Journal of Physical Chemistry. B. 2004;**108**(23):7728-7734. DOI: 10.1021/jp049495v
- [32] Moisala A, Nasibulin AG, Kauppinen EI. The role of metal nanoparticles in the catalytic production of single-walled carbon nanotubes—A review. Journal of Physics: Condensed Matter. 2004;**15**(42):1-26. DOI: 10.1088/0953-8984/15/42/003
- [33] Park J-B, Choi G-S, Cho Y-S, et al. Characterization of Fe-catalyzed carbon nanotubes grown by thermal chemical vapor deposition. Journal of Crystal Growth. 2002;**244**(2):211-217. DOI: 10.1016/S0022-0248(02)01661-5
- [34] Yamada T, Namai T, Hata K, et al. Size-selective growth of double-walled carbon nanotube forests from engineered iron catalysts. Nature Nanotechnology. 2006;**1**(2):131-136. DOI: 10.1038/nnano.2006.95
- [35] Ho GW, Wee ATS, Lin J, Tjiu WC. Synthesis of well-aligned multiwalled carbon nanotubes on Ni catalyst using radio frequency plasma-enhanced chemical vapor deposition. Thin Solid Films. 2001;**388**(1-2):73-77. DOI: 10.1016/S0040-6090(01)00828-8
- [36] Ren ZF, Huang ZP, Wang DZ, et al. Growth of a single freestanding multiwall carbon nanotube on each nanonickel dot. Applied Physics Letters. 1999;**75**(8):1086-1088. DOI: 10.1063/1.124605
- [37] Bethune DS, Kiang CH, de Vries MS, et al. Cobalt-catalysed growth of carbon nanotubes with single-atomic-layer walls. Nature. 1993;**363**(6430):605-607. DOI: 10.1038/363605a0
- [38] Teo KBK, Chhowalla M, Amaratunga GAJ, et al. Uniform patterned growth of carbon nanotubes without surface carbon. Applied Physics Letters. 2001;**79**(10):1534-1536. DOI: 10.1063/1.1400085
- [39] Wen H-C, Yang K, Ou K-L, Wu W-F, Luo R-C, Chou C-P. Carbon nanotubes grown using cobalt silicide as catalyst and hydrogen pretreatment. Microelectronic Engineering. 2005;**82**(3-4):221-227. DOI: 10.1016/j.mee.2005.07.028
- [40] Thomas Koilraj T, Kalaichelvan K. Synthesis of carbon nanotubes using Fe-Mo/AL<sub>2</sub>O<sub>3</sub> bimetallic catalyst by CVD method. IEEE-International Conference on Advanced Engineering Science and Management (ICAESM-2012). 2012:429-433
- [41] Jeong SW, Son SY, Lee DH. Synthesis of multi-walled carbon nanotubes using Co-Fe-Mo/Al<sub>2</sub>O<sub>3</sub> catalytic powders in a fluidized bed reactor. Advanced Powder Technology. 2010;**21**(2):93-99. DOI: 10.1016/j.appt.2009.10.008
- [42] He M, Chernov AI, Obraztsova ED, Jiang H, Kauppinen EI, Lehtonen J. Synergistic effects in FeCu bimetallic



catalyst for low temperature growth of single-walled carbon nanotubes. Carbon. 2013;**52**:590-594. DOI: 10.1016/j.carbon.2012.10.029

[43] Pesetski AA, Baumgardner JE, Krishnaswamy SV, et al. A 500 MHz carbon nanotube transistor oscillator. Applied Physics Letters. 2008;**93**(12):123506. DOI: 10.1063/1.2988824

[44] Chen Q, Yuan X, Cole M, Zhang Y, Meng L, Yan Y. Theoretical study of a 0.22 THz backward wave oscillator based on a dual-gridded, carbon-nanotube cold cathode. Applied Sciences. 2018;**8**(12):2462. DOI: 10.3390/app8122462

[45] Il'ina MV, Il'in OI, Blinov YF, Smirnov VA, Ageev OA. Nonuniform elastic strain and memristive effect in aligned carbon nanotubes. Technical Physics. 2018;**63**(11):1672-1677. DOI: 10.1134/S1063784218110129

[46] Ilina MV, Blinov YF, Ilin OI, Rudyk NN, Ageev OA. Piezoelectric effect in non-uniform strained carbon nanotubes. IOP Conference Series: Materials Science and Engineering. 2017;**256**:012024. DOI: 10.1088/1757-899X/256/1/012024

[47] Rudyk NN, Il'in OI, Il'ina MV, Fedotov AA, Klimin VS, Ageev OA. Carbon nanotubes based vacuum gauge. Journal of Physics Conference Series. 2017;**917**:082008. DOI: 10.1088/1742-6596/917/8/082008

[48] Xiao Z, Kong LB, Ruan S, et al. Recent development in nanocarbon materials for gas sensor applications. Sensors and Actuators B: Chemical. 2018;**274**:235-267. DOI: 10.1016/j.snb.2018.07.040

[49] Zhbanov A, Pogorelov E, Chang Y-C. Carbon nanotube field emitters.

In: Carbon Nanotubes. IntechOpen. London, UK; 2010. DOI: 10.5772/39432

[50] Yan X, Wu Y, Wang B, et al. Fabrication of carbon nanotube on nickel–chromium alloy wire for high-current field emission. Applied Surface Science. 2018;**450**:38-45. DOI: 10.1016/j.apsusc.2018.04.114